Finite Element Analysis of Reinforced Concrete Continuous Beams Strengthened by External Layers

Khaled M. Heiza

Civil Engineering Department, Menoufiya University, Egypt

E-mail: khheiza@ yahoo.com, khheiza@ hotmail.com

Abstract: Repair and strengthening of the existing constructions are very essential in many cases and may be the sole right decision. A computer program based on the finite element method has been developed and a new compound element was used to simulate the reinforced concrete members strengthened with external layers on the different sides. Each compound element consists of four sub-elements. The sub-elements are two dimensional isoparametric degenerated elements with eight nodes and five degrees of freedom. Each sub element consists of different concrete, steel and strengthening laminates. Seven models from an experimental test program of RC beams strengthened with external layers in different sides were analyzed by the finite elements. The new developed compound element has been proved to be capable to solve any reinforced concrete member strengthened with additional external layers at different sides with accurate representations and acceptable results.

[KHALED M. HEIZA. Finite Element Analysis of Reinforced Concrete Continuous Beams Strengthened **by External Layers**. Journal of American Science 2011;7(10):631-644]. (ISSN: 1545-1003).

http://www.americanscience.org.

Keywords: Finite element, compound element, strengthening, isoparametric, bending stresses, plane stresses.

1. Introduction

The finite element method is firmly established as an engineering tool of wide applicability [1, 2 and 3]. Reinforced concrete structures are now analyzed by the finite elements in wide ranges. Defects of structures may appear due to unexpected conditions such as overloading, mistakes in the design or construction. Traditional and advanced materials are used to repair and for strengthening such structures. Simulating the real case of these structures by some analytical models will help the researchers to analyze many constructions with vast variable cases. Reinforced concrete structures can be modeled by using layered plane stress elements which is suitable in case of shear failure problems [4,5], bending stress elements which is suitable in case of flexural failure problems [6,7] or by three dimensional elements [8,9]. In this research, a new constitutive model has been developed to analyze different reinforced concrete members with their additional strengthening layers in any direction and can represent both plane stresses and bending stresses in order to simulate the actual case. This model was compared with the other techniques of the layered finite element analysis. The suggested model was also verified by comparing the analytical results with the experimental results for reinforced concrete beams strengthened by steel plates, and glass fibers wraps as additional external strengthening layers [10-13]. These beams were analyzed by the new constitutive modes to simulate such layers in different positions.

2. Finite Element Method

Development of appropriate methods for the analysis of reinforced concrete structures considering the different nonlinear effects is increasingly demanded to ensure the safety of the design. The finite element method is considered as an important engineering tool to analyze most of these problems. The basic concept of this method was fully explained and documented in details for different procedures and techniques in many references [1, 3]. Although finite element procedures have been applied to concrete structures for over fifty years, the search for suitable elements as well as considering the material and geometrical nonlinear properties are still in progress and enhancement.

The elements degenerated from the three dimensional elements were introduced by Hinton [2] to the nonlinear analysis of reinforced concrete plates and shells. The results were satisfactory for both thin and thick thicknesses. In the present analysis, isoparametric degenerated layered elements of independent rotational and displacement degrees of freedom were employed. The main feature of the chosen element and the nonlinear procedure will be reviewed briefly.

2.1 Reissner-Mindlin Theory

Transverse shear deformations have some effects on the behavior of plates. These effects increase as the thickness of the plate increases. The main theories for the analysis of plates are: Kirchhoff classical thin plate theory and Reissner-Mindlin plate theory [5]. In Mindlin theory, transverse shear deformations are considered which permit the applications for both thin and thick plates or shells. Fig. 1 shows both theories. The main assumptions are:

(I) displacements are small compared with the plate thickness,

(II) the stress normal to the mid-surface of the plate is negligible,

(III) normals to the mid-surface before deformation remain straight but not necessarily normal to the mid-surface after deformation.

The main displacement parameters can be expressed as follows:

$$u=(x,y,z)=z\,\theta_x(x,y),\quad v=(x,y,z)=z\,\theta_y(x,y),\quad w=(x,y,z)=w(x,y) \tag{1}$$

Where: u, v, w are the displacements in x, y, z directions respectively, (x, y) are the coordinates in the plan, z: is the thickness direction coordinate, w: is the mid-plane displacement, and (θ_x, θ_y) are the rotations of the normals in the xz and yz planes respectively due to bending and can be defined by the following equations:

$$\theta_x=\frac{\partial w}{\partial x}-\phi_x\ ,\qquad \theta_y=\frac{\partial w}{\partial y}-\phi_y\ , \tag{2}$$

Where: ϕ_x, ϕ_y are the shear rotations.

2.2. Isoparametric DegeneratedElement

A special formulations based on a degenerate three dimensional element [2] were applied with the following assumptions:

(I) for thick plates, normals to the middle surface remain straight after deformations,

(II) the strain energy corresponding to stresses perpendicular to the middle surfaces is ignored.

With these assumptions, which agree with the assumptions of the Reissner-Mindlin theory, an efficient tool for analyzing both thin and thick plates or shells becomes available This method enabled the shell element to represent the other thick structurs such as walls, beams and columns. Fig. 2 shows both the three dimensional element and the corresponding degenerated shell element.

Geometric definitions of the element: The relation between the Cartesian coordinates of any node and the curvilinear coordinates can be written for 8-node degenerated element as follows:

$$\begin{Bmatrix}x\\y\\z\end{Bmatrix}=\sum_{i=1}^{8}N_i(\xi,\eta)\begin{Bmatrix}x_i\\y_i\\z_i\end{Bmatrix}_{mid.}+\sum_{i=1}^{8}N_i(\xi,\eta)\frac{\zeta}{2}V_{3i}, \tag{3}$$

Where: V3i is a vector constructed from the nodal coordinates of the top and bottom surfaces at the node i as shown in Fig. 3(a),

$$V_{3i}=\begin{Bmatrix}x_i\\y_i\\z_i\end{Bmatrix}_{top}-\begin{Bmatrix}x_i\\y_i\\z_i\end{Bmatrix}_{bottom}, \tag{4}$$

Ni (ξ,η) are the shape functions and ξ, η, ζ are the curvilinear coordinates of the point. The geometry and the assumed displacement field were identified with the same functions which characterize the isoparametric element. The shape functions for the eight boundary nodes are shown in Fig. 3(b) which are serendipity shape functions and can be defined by the following equations:

(I) For corner nodes (i = 1, 3, 5, 7)

$$N_i=\frac{1}{4}(1+\xi\xi_i)(1+\eta\eta_i)(\xi\xi_i+\eta\eta_i-1). \tag{5}$$

(II) For mid-side nodes (i = 2, 4, 6, 8)

$$N_i=\frac{\xi_i^2}{2}(1+\xi\xi_i)(1-\eta^2)+\frac{\eta_i^2}{2}(1+\eta\eta_i)(1-\xi^2). \tag{6}$$

Displacements: The displacement field is described by the five degrees of freedom; the three displacements of the mid-surface node (u, v, w) and two rotations (α_i , β_i) as follows:

$$\begin{Bmatrix}u\\v\\w\end{Bmatrix}=\sum_{i=1}^{8}N_i(\xi,\eta)\begin{Bmatrix}u_i\\v_i\\w_i\end{Bmatrix}_{mid.}+\sum_{i=1}^{8}N_i(\xi,\eta)\frac{\zeta h_i}{2}[V_{1i}-V_{2i}]\begin{Bmatrix}\alpha_i\\\beta_i\end{Bmatrix}, \tag{7}$$

Where: h_i is the thickness of the element at the node i ;

$$V_{1i}=i\times V_{3i}\ ,\qquad V_{2i}=V_{1i}\times V_{3i}, \tag{8}$$

in which i is the unit vector in the x-direction.

Layered discretization: The finite element is divided into a number of concrete, steel, and any additional repair or strengthening layers.

The entire element stiffness was obtained by summing up the stiffness of the layers [3]. The stresses were computed at the mid-surface of the layer and assumed to be constant over the thickness of each layer as shown in Fig. 4.

The layer thickness was defined in terms of curvilinear coordinate ζ to permit the variation of the layer thickness as the element thickness varies as shown in fig.5. The stiffness of the element K^e was obtained by numerical integration through the thickness:

$$\underline{k}^e=\iiint \underline{B}^T\underline{D}\,\underline{B}\,J\,d\zeta\,d\xi\,d\eta, \tag{9}$$

$$\underline{f}^e=\iiint \underline{B}^T\underline{\sigma}\,J\,d\zeta\,d\xi\,d\eta, \tag{10}$$

Where: B is the strain matrix composed of derivatives of the shape functions, J: determinant of the Jacobian matrix.

2.3. New Compound Finite Element

A new compound finite element was constructed from four isoparametric degenerated layered elements to account for both flexure and shear stresses for RC members with rectangular cross-section. The new finite element consists of two finite elements with layers parallel to the top surface E1, E3 and another two finite elements with layers parallel to the sides of the member E2, E4 as shown in Fig. 6. The combination between the four sub elements E1, E2, E3, and E4 forms the new elements. The developed compound element can easily represent both plane stresses in sub elements E2, E4 as well as bending stresses in sub elements E1 and E3. Also, this facilitates representing strengthening layers in the required directions. The

dimensions of the finite element were defined in terms of curvilinear coordinate's ξ, η and ζ to permit the variation of the thickness, the width and the length of the layers.

Each node of the sub element was specified by three coordinates X, Y, Z for both the top and the bottom surfaces to form the thickness of the element at the node. This gives the facility of representing the structure in the space. The stiffness of the new compound element K^e was obtained by numerical integration through the thickness equation (9):

The stress resultants were calculated by the integration of the stress components at the mid-layers:

(I) Normal forces

$$N_x = \int_{-h/2}^{+h/2} \sigma_x \, dz = \frac{h}{2} \sum_{i=1}^{n} \sigma_x^i \Delta\zeta^i,$$

$$N_y = \int_{-h/2}^{+h/2} \sigma_y \, dz = \frac{h}{2} \sum_{i=1}^{n} \sigma_y^i \Delta\zeta^i. \quad (11)$$

(II) Shear forces

$$Q_x = \int_{-h/2}^{+h/2} \tau_{xz} \, dz = \frac{h}{2} \sum_{i=1}^{n} \tau_{xz}^i \Delta\zeta^i,$$

$$Q_y = -\int_{-h/2}^{+h/2} \tau_{yz} \, dz = -\frac{h}{2} \sum_{i=1}^{n} \tau_{yz}^i \Delta\zeta^i. \quad (12)$$

(III) Bending moments

$$M_x = -\int_{-h/2}^{+h/2} \sigma_x \, z dz = -\frac{h}{4} \sum_{i=1}^{n} \sigma_x^i \zeta^i \Delta\zeta^i,$$

$$M_y = -\int_{-h/2}^{+h/2} \sigma_y \, z dz = -\frac{h}{4} \sum_{i=1}^{n} \sigma_y^i \zeta^i \Delta\zeta^i, \quad (13)$$

$$M_{xy} = -\int_{-h/2}^{+h/2} \tau_{xy} \, z dz = -\frac{h}{4} \sum_{i=1}^{n} \tau_{xy}^i \zeta^i \Delta\zeta^i, \quad (14)$$

Where: n is the total number of layers, and h is the thickness of the element.

2.4. Nonlinear Material Properties

The finite element technique permits a more realistic analysis for reinforced concrete complexities which arise from concrete cracking, tension stiffening, nonlinear multiaxial material properties and complex interface behavior. In the present study, both the perfect and the strain-hardening plasticity approach were considered to model the compressive behavior of the concrete. The flow theory of plasticity [5] was employed to establish the nonlinear stress-strain relations in the plastic range.

Yielding criterion for concrete: The yielding criterion for concrete under a triaxial state is generally depending on the three stress invariants. For most cases, the mean normal stress I_1 and the shear stress invariant J_2 are adequate to define the yield criterion [5].

$$f(I_1, J_2) = [\beta(3J_2) + \alpha I_1]^{\frac{1}{2}} = \sigma_o, \quad (15)$$

Where: σo is the equivalent effective stress taken as the compressive stress from uniaxial tests, and α, β are two material parameters. The Von-Mises yield criterion [5] assumes that α = 0.0 and β = 1.0. The relation between the equal biaxial yield stress f_{cb} and the uniaxial yield stress f_c' may be assumed as:

$$f_{cb} = 1.16 f_c' \quad (16)$$

Applying Kupfer's results [11] yields that α= 0.355 σ_o and β= 1.355. So, equation (15) can be written in terms of the stress components as:

$$f(\sigma) = \{1.355[(\sigma_x^2 + \sigma_y^2 - \sigma_x\sigma_y) + 3(\tau_{xy}^2 + \tau_{xz}^2 + \tau_{yz}^2)] + 0.335\sigma_o(\sigma_x + \sigma_y)\}^{\frac{1}{2}} = \sigma_o \quad (17)$$

In the perfect plastic model, σ_o was taken as the ultimate stress f_c' obtained from uniaxial compression tests. When the effective stress reaches the ultimate stress f_c' a perfectly plastic response is assumed until the crushing surface is reached.

Concrete crushing: The crushing of the concrete is considered as a strain controlled phenomenon. The appropriate strain criterion may be developed by converting the yield criterion defined in terms of stresses (Eq. 15) directly into strains:

$$f'(I_1', J_2') = [\beta(3J') + \alpha I']^{\frac{1}{2}} = \varepsilon_u, \quad (18)$$

Where: I_1' and J_2' are strain invariants and ε_u is the ultimate strain.

Applying the material parameters determined from Kupfer's results, the crushing condition is expressed in terms of the total strain components as follows:

$$f'(\varepsilon) = \{1.355[(\varepsilon_x^2 + \varepsilon_y^2 - \varepsilon_x\varepsilon_y) + 0.75(\gamma_{xy}^2 + \gamma_{xz}^2 + \gamma_{yz}^2)] + 0.335\varepsilon_u(\varepsilon_x + \varepsilon_y)\}^{\frac{1}{2}} = \varepsilon_u. \quad (19)$$

The concrete is assumed to loose all of its characteristics of strength and rigidity when ε_u reaches the value of the ultimate strain.

Concrete cracking: Cracks are formed in any of the concrete layers when the tensile stress at a principal direction reaches the value of f_t', and developed in the direction normal to that principal stress. Assuming 1 and 2 are the two principal directions in the plane of the structure and 3 is perpendicular to this plane, the stress-strain relationship for concrete which is cracked in the first principal direction, is:

$$\begin{bmatrix}\sigma_1\\ \sigma_2\\ \tau_{12}\\ \tau_{13}\\ \tau_{23}\end{bmatrix}=\begin{bmatrix}0&0&0&0&0\\ 0&E&0&0&0\\ 0&0&G_{12}^c&0&0\\ 0&0&0&G_{13}^c&0\\ 0&0&0&0&G_{23}^c\end{bmatrix}\begin{bmatrix}\varepsilon_1\\ \varepsilon_2\\ \gamma_{12}\\ \gamma_{13}\\ \gamma_{23}\end{bmatrix}, \quad (20)$$

Where: G_{ij}^c is the cracked shear modulus as a function of the current tensile strain represented as follows:

$$G_{12}^c=0.25G(1-\frac{\varepsilon_1}{0.004});\ G_{12}^c=0.0,\ \text{if}(\varepsilon_1\ge 0.004), \quad (21)$$
$$G_{13}^c=G_{12}^c,\quad G_{23}^c=\frac{5G}{6},\quad \text{and } G=\frac{E}{2(1+\nu)}.$$

When cracks develop in both the principal directions, the stress-strain relationship becomes:

$$\begin{bmatrix}\sigma_1\\ \sigma_2\\ \tau_{12}\\ \tau_{13}\\ \tau_{23}\end{bmatrix}=\begin{bmatrix}0&0&0&0&0\\ 0&0&0&0&0\\ 0&0&G_{12}^c&0&0\\ 0&0&0&G_{13}^c&0\\ 0&0&0&0&G_{23}^c\end{bmatrix}\begin{bmatrix}\varepsilon_1\\ \varepsilon_2\\ \gamma_{12}\\ \gamma_{13}\\ \gamma_{23}\end{bmatrix}, \quad (22)$$

where G_{ij}^c is defined as:

$$G_{13}^c=0.25G(1-\frac{\varepsilon_1}{0.004});\quad G_{13}^c=0.0,\ \text{if}(\varepsilon_1\ge 0.004),$$
$$G_{23}^c=0.25G(1-\frac{\varepsilon_2}{0.004});\quad G_{23}^c=0.0,\ \text{if}(\varepsilon_2\ge 0.004), \quad (23)$$
$$G_{12}^c=0.5G_{13}^c;\quad \text{or } G_{12}^c=0.5G_{23}^c,\ \text{if } (G_{23}^c<G_{13}^c).$$

Modeling of steel: The reinforcing bars were replaced by an equivalent "smeared" distributed steel layer. The equivalent thickness of the steel layer is given by:

$$t_s=\frac{A_s}{b}=\mu\times d, \quad (24)$$

Where: A_s is the cross-sectional area of one reinforcing bar, b is the spacing of the bars, μ is the reinforcement ratio and d is the effective depth.

The thicknesses of the steel layers and the effective depths were specified in the analysis by the curvilinear coordinate ζ. Each steel layer has uniaxial behavior, resisting only axial forces in the bar direction.

Tension stiffening: Fig. 7 shows the stress distribution of a cracked reinforced concrete element. As the load increases, more cracks develop and the amount of the tension carried by the concrete is gradually decreased. A gradual release of the concrete stress component normal to the cracked plane was considered in the present work as shown in Fig. 8. The modulus of elasticity is decreased due to cracking as strain increase by following the formula:

$$E_i=\frac{\alpha f_t^{'}}{\varepsilon_i}(1-\frac{\varepsilon_i}{\varepsilon_m});\ \varepsilon_t\le\varepsilon_i\le\varepsilon_m \quad (25)$$

Where: f_t' is the modulus of rupture of the concrete and α, ε_m : aretension stiffening parameters.

The normal stresses are obtained by:

$$\sigma_1=\alpha f_t^{'}(1-\frac{\varepsilon_1}{\varepsilon_m});\ \varepsilon_t\le\varepsilon_1\le\varepsilon_m,\quad \sigma_2=\alpha f_t^{'}(1-\frac{\varepsilon_2}{\varepsilon_m});\ \varepsilon_t\le\varepsilon_2\le\varepsilon_m. \quad (26)$$

3. Computer Program

The finite element program developed in this work is an extended version of the program given in Ref. [7]. Isoparametric degenerated layered elements of eight nodes per element and five degrees of freedom per each node were chosen. Material nonlinearities for both the concrete and the steel were taken into account as well as geometrical nonlinearity. The modified Newton-Raphson method was applied in the analysis [1]. The tangential stiffness matrix was recalculated for the second iteration of each load increment. The main features of the program are summarized as follows:

1. The large input data file required for the new compound elements mesh is reduced by developing a general mesh generator which creates all the required data for the compound elements.
2. Each node of the element is specified by three coordinates X, Y, Z for both the top and the bottom. This gives the facility of representing the structure in the space. Top and bottom coordinates of each node enable to define the top and bottom surface of the element and to represent any variation of the thickness through the element.
3. The material properties of the concrete, steel, or strengthening layers can be modified for any element to provide the best simulation of the strengthened RC structure.
4. The dimensions of the finite element are defined in terms of curvilinear coordinates ζ, η, and ξ to permit the variation of the thickness, the width and the length of the layers.
5. The created compound element can easily represent both plane stresses and bending stresses in sub elements as well as reinforcement and strengthening layers in the required directions.
6. To identify the stresses and strains inside the element, 3x3 Gauss points have to be considered to define the stresses and strains at each layer of the element.

Fig. 9, present the procedure of the analysis in the program.

4. Application Example

An experimental program was carried out to investigate the behavior of two-span continuous self-compacting reinforced concrete beams repaired and strengthened using both the traditional and the advanced materials by different techniques [7]. The

experimental program consists of twenty-two of reinforced concrete beam models which have a constant cross section and reinforcement as shown in Fig. 10.

Cases of study: The following cases were chosen from the experimental program [7].

Case (a): One RC beam without strengthening, control beam Bo.

Case (b): Two RC beams strengthened with steel plates or GFRP on top and bottom surfaces (BSSTB and BSGTB).

Case (c): Two RC beams strengthened with steel plates or GFRP on both vertical sides at +ve moments, (BSS+ve|| and BSG+ve||).

Case (d): Two RC beams repaired with steel plates or GFRP at U shape at the bottom surface and on both vertical sides after preloading level =50% of the failure load of Bo, (BRSU and BRGU).

Fig. 10 shows the investigated cases (b, c, and d) for the different strengthening techniques.

The material properties of the test program were introduced in the table 1.

Different cases of study were analyzed by the FEM to show the efficiency of using the new compound model for the analysis of reinforced concrete beams strengthened in different directions as shown in fig.11. The results were compared with the experimental results for both the plane stress and bending stress finite element techniques.

Modeling of tested beams by FEM: For the symmetry, only one half of the beam is analyzed considering fixation at the intermediate support. Fig. 12 shows the capability of bending, plane stress and compound layered elements for representing the real RC section strengthened with additional external layers from all sides. It was noticed that bending stress layered element cannot represent the vertical legs of stirrups and side strengthening layers. The plane stress layered element cannot represent the horizontal legs of stirrups and the top and bottom strengthening layers. However, the new compound element can represent all reinforcements as well as the all strengthening layers.

The tested beams were modeled by three different techniques, as shown in Fig. 13. The first one performed by using nine bending stress elements with 48 nodes and the second by using 45 plane stress elements with 164 nodes while the third was by using nine new compound elements consists of 36 sub elements with 116 nodes. The generated mesh used for the analysis and the boundary conditions for the different techniques are shown in Fig. 13. Loads are applied in one ton increments to simulate the same procedure as for the experiments. Deflections, stresses, strains, cracking of the concrete, yielding of reinforcements or strengthening steel plates, or failure of the GFRP layers were all recorded by the analysis. The load deflection curves can express the overall behavior of the beam correctly. In this research, only the load deflection curves will be compared for different cases by the different methods.

Analysis of the results: Case (a): Load deflection curves of the experimental and analytical results for the RC control beam Bo are compared in Fig. 14. The finite element results showed a good correlation with the experimental results. The new model shows the best representation of the control RC beam. The results of the bending stress techniques can be improved with increasing the number of elements.

In Case (b): As the RC beams are strengthened on the top and bottom surfaces, beams can be analyzed by bending stress elements and the compound elements. Figs. 15 and 16 show the load deflection curves for both the numerical methods and the experimental results for beams which have been strengthened with steel plates and GFRP respectively. The results of the new compound elements can be considered as the best results with respect to the experimental results.

In Case (C), if the RC beams strengthened with steel plates or GFRP on both vertical sides at +ve moments, beams can be analyzed by plane stress elements and the compound elements. Figs. 17 and 18 compare the load deflection curves for both the numerical methods and the experimental results for beam strengthened with steel plates and GFRP respectively. The results of the new compound elements agree with the experimental results.

Case (d) represents RC beams that have been repaired by steel plates or GFRP as U shape at the bottom surface and on both vertical sides after preloading level =50% of the failure load of Bo. Beams can only be analyzed by the new compound elements. Figs. 19 and 20 compare the load deflection curves of the numerical method with the experimental results for beam strengthened with steel plates and GFRP respectively. The results of the new compound elements showed a good correlation and harmony with the experimental results.

From this analysis, it is found that the new compound model had been proven to be capable of representing the RC beams with any strengthening layers in any directions and can estimate the behavior with a good accuracy.

5. Conclusions

From this research the following conclusions may be drawn:

1. The quadrilateral isoparametric degenerated shell element applied in this research work can perform the analysis of 3D-structures efficiently, where each node of the element has top and bottom coordinates and is specified in X, Y, Z directions.

2. The degenerated element which is based on a degenerated three dimensional continuum element permits to represent any variation of the thickness in the element. Subsequently, any variation in the thickness of the structure can be simulated
3. The discrete layered approach enables to cover variable material properties of reinforced concrete structures not only along the surface of the structure but also through the thickness.
4. Considering the shear deformations by applying Reissner-Mindlin theory in the analysis enables to analyse both thin and thick elements.
5. The developed new compound element can easily represent both plane stresses and bending stresses in sub elements that facilitate to represent the reinforcement as well as the strengthening layers in the required sides.
6. The new compound element showed good correlation and harmony with the test results which can help for predicting the behavior of repair and strengthened structures. More different cases with new different parameters can be studied and investigated easily.
7. The developed integrated computer program based on the new compound finite elements had been proved to be capable for the numerical analysis of the nonlinear behavior of strengthened RC members. The results of the tested beams had verified the reliability of this developed model to simulate the nonlinear behavior of reinforced concrete beams strengthened with external layers in any directions.

List of Symbols

is the compressive strength of the self compact concrete	fc'
is the modulus of rupture of concrete	ft'
is the young's modulus of concrete	Ec
is the young's modulus of steel	Es
is the yield stress of the normal mild steel	fy
is the yield stress of the high tensile steel	fy
is the yield stress of the steel plate used for strengthening	fy
is the tensile modulus of the used GFRP wraps	E
is the tensile strength of the used GFRP wraps	σ
are the displacements in x, y, z directions respectively	u, v, w
are the coordinates in the plan	x, y
is the thickness direction coordinate	z
is the mid-plane displacement	w
are the rotations of the normals in the xz and yz planes respectively	θ_x, θ_y
is the shear rotations	ϕ_x , ϕ_y
is a vector constructed from the nodal coordinates	V3i
are the shape functions	Ni
are the curvilinear coordinates of the point	ξ, η, ζ
is the thickness of the element	h_i
The unit vector in the x-direction	i
is the stiffness of the element	K^e
is strain matrix	B
is the determinant of the Jacobian matrix	J
is the total number of layers	n
is the thickness of the element.	h
is the equivalent effective stress	σo
are two material parameters	α, β
are strain invariants	I_1', J_2'
is the ultimate strain.	ε_u
is the cracked shear modulus	G_{ij}^c
is the modulus of rupture of the concrete	f_t'
is the cross-sectional area	A_s

Table 1: material properties of the test program [7]

property	Symbol	Value (MPa)
Compressive strength of the self compact concrete	fc'	50
Modulus of rupture of concrete	ft'	3.2
Young's modulus of concrete	Ec	23000
Young's modulus of steel	Es	210000
Yield stress of the normal mild steel	fy	240
Yield stress of the high tensile steel	fy	360
Yield stress of the steel plate used for strengthening	fy	235
Tensile modulus of the used GFRP wraps (Hex-100 G)	E	70000
Tensile strength of the used GFRP wraps (Hex-100 G)	σ	2294.4

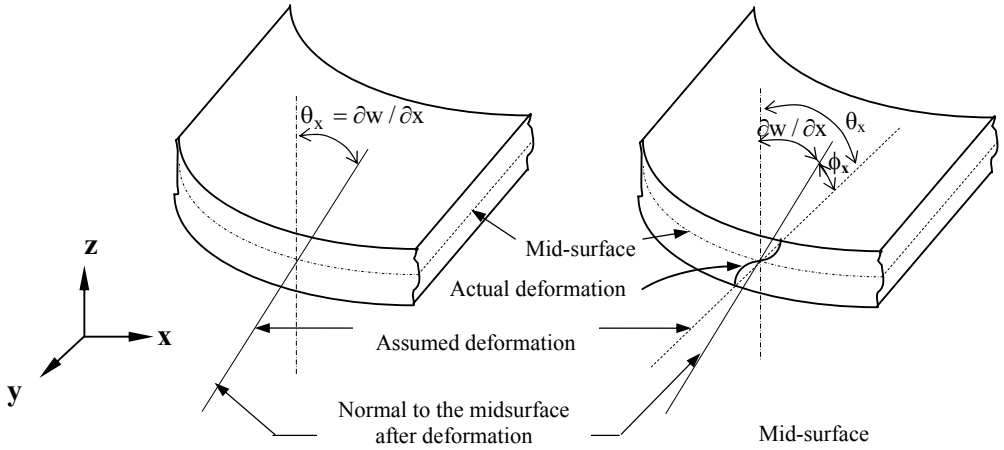

(a) Kirchhoff assumptions (b) Mindlin assumptions

Fig. 1. Deformation of the cross-section of the shell element

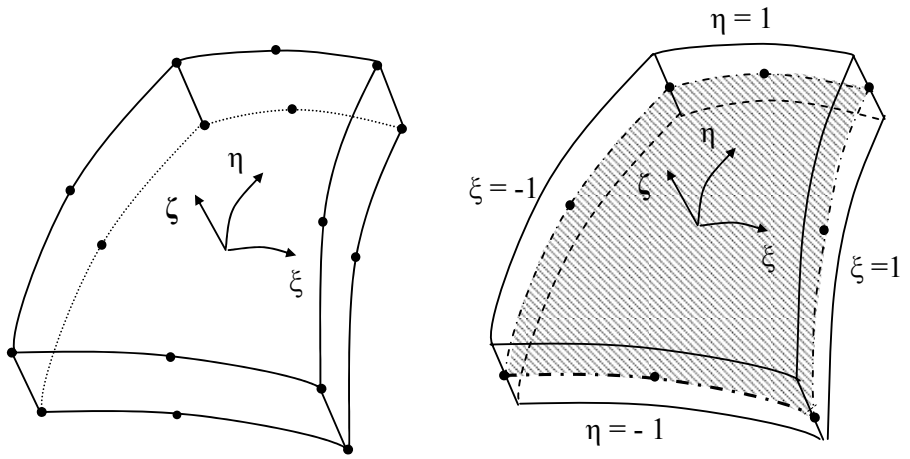

(a) 3D-element (16 nodes) (b) Degenerated element (8 nodes)

Fig. 2. Degeneration of 16 nodes 3D-element to 8 nodes shell element [2]

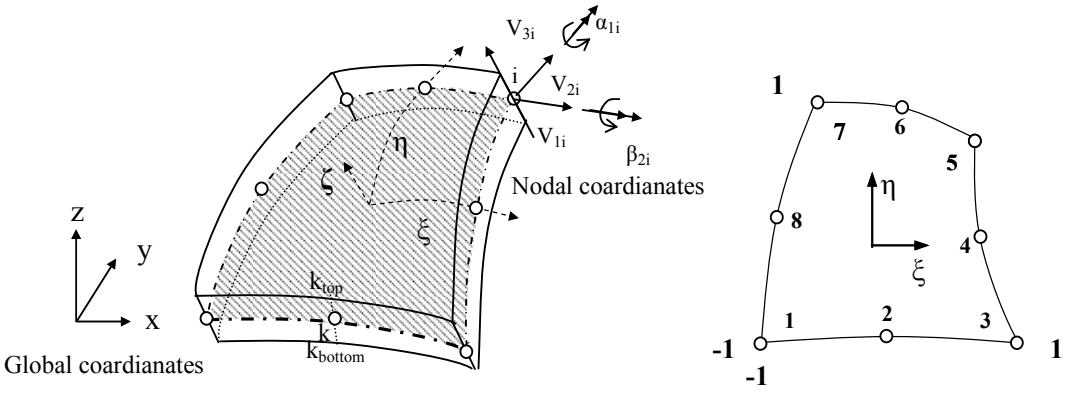

(a) Loacal and global coardianates (b) Isoparametric element

Fig. 3. Coordinate systems for isoparameteric degenerated element

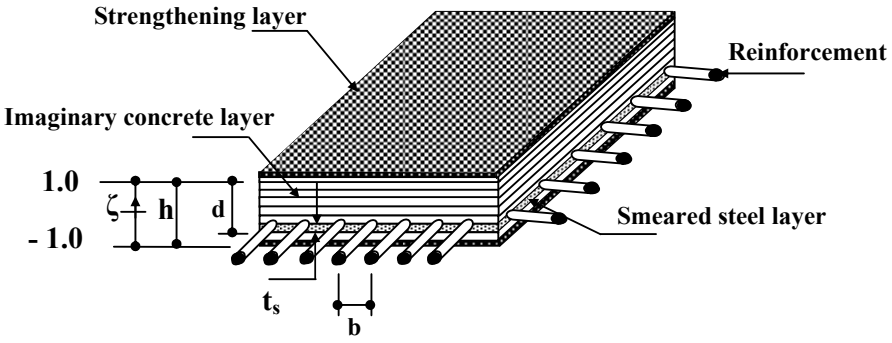

Fig. 4. Reinforced concrete element with strengthening layers

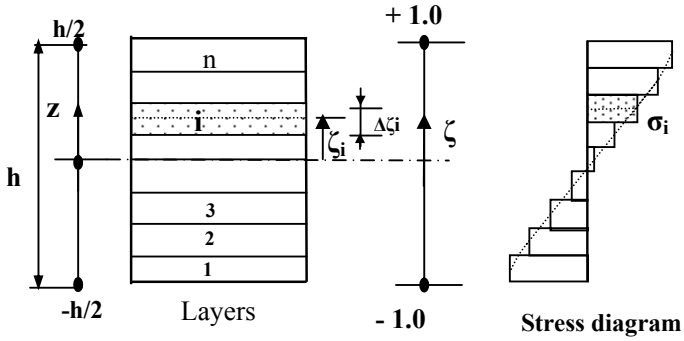

Fig. 5. Layered element; curvlinear coardinate and stress diagram

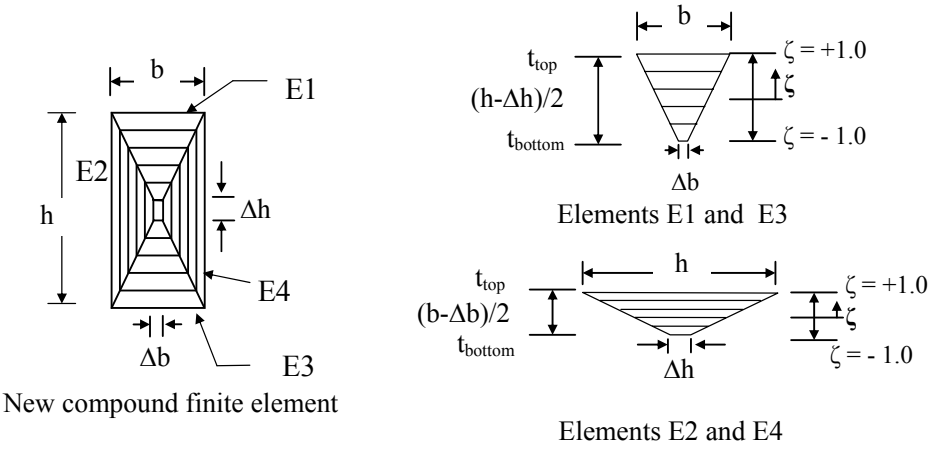

Fig. 6. Details of the new compound finite element

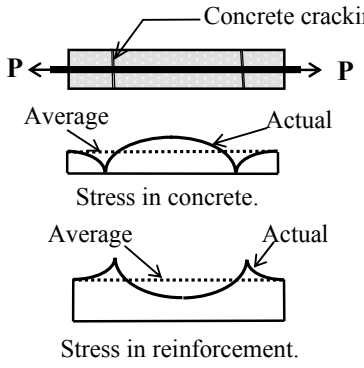

Fig. 7. Stresses in cracked RC element

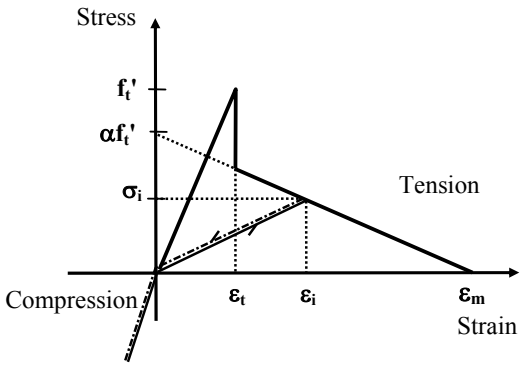

Fig. 8. Tension stiffening model [3]

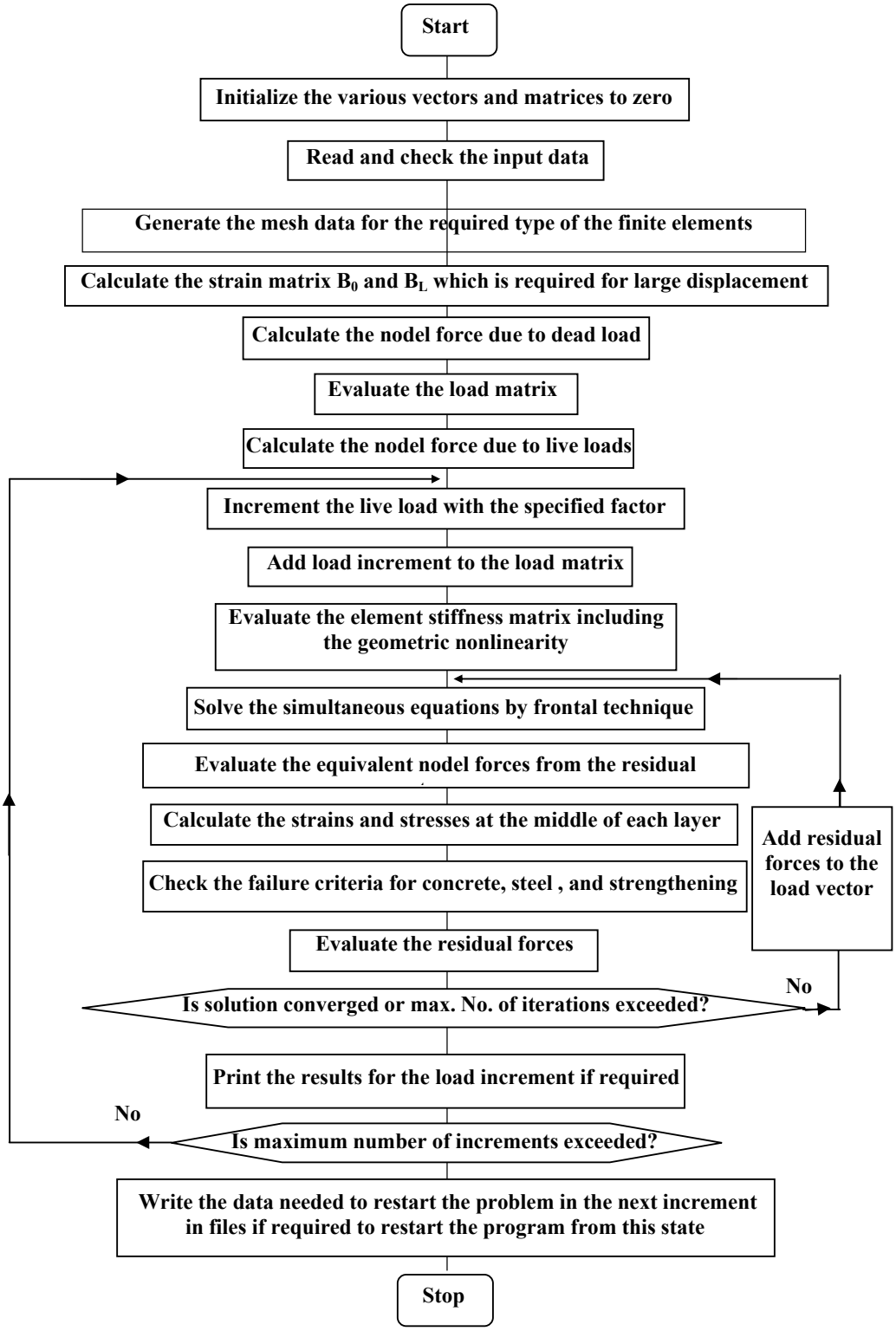

Fig. 9 Flowchart of the computer program

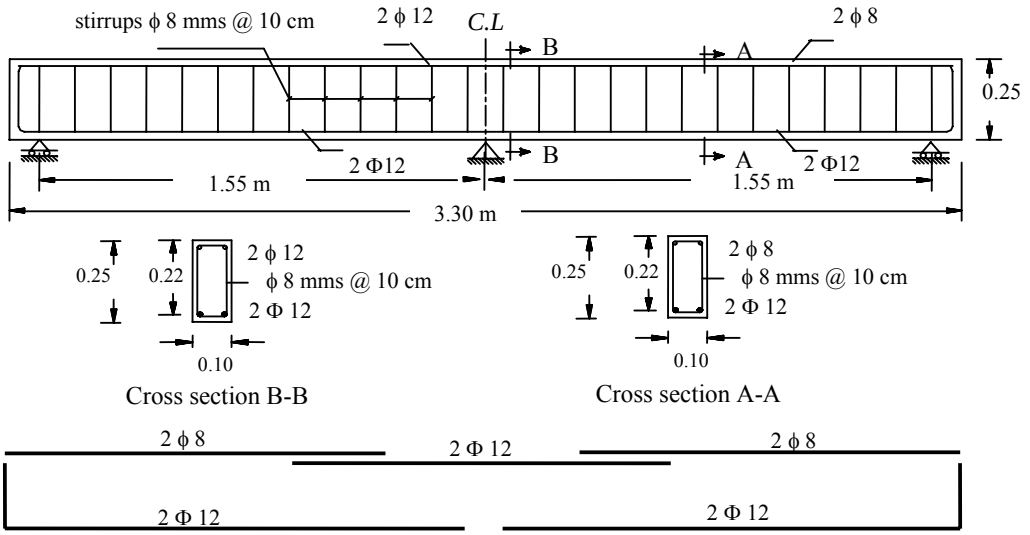

Figure 10. Typical dimensions and details of reinforcement of the control beam B_o

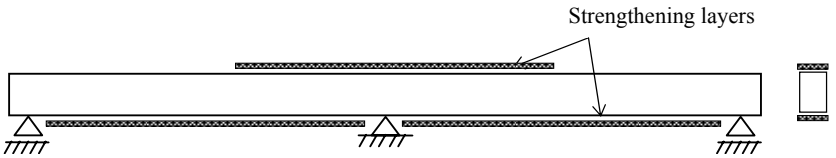

Case (b): Strengthening on top & bottom surfaces (BSSTB and BSGTB)

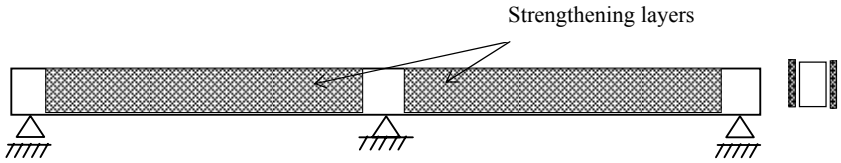

Case (c): Strengthening on vl. sides at +ve moments (BSS+ve|| and BSG+ve||)

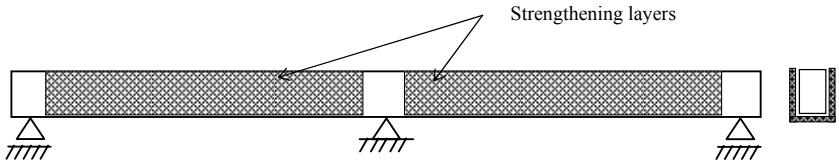

Case(d): Repairing with **U**-shape at +ve moments (BRSU and ,BRGU)

Fig. 11. Strengthening schemes by steel plates and GFRP [7]

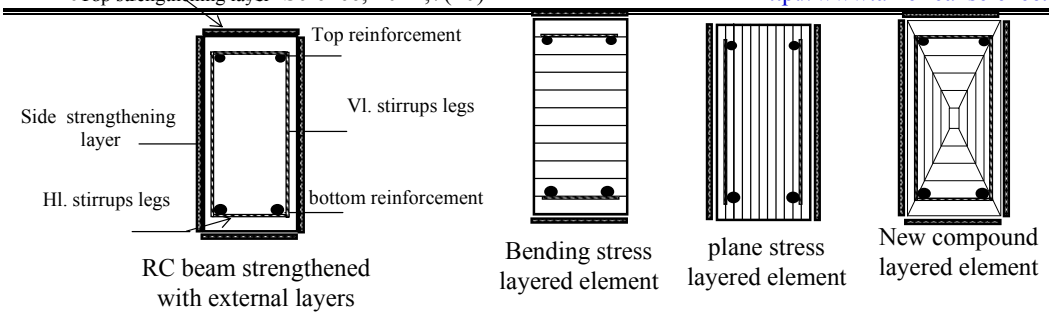

Fig. 12. Reinforcement and strengthening layers that can be represented by different techniques of the finite elements

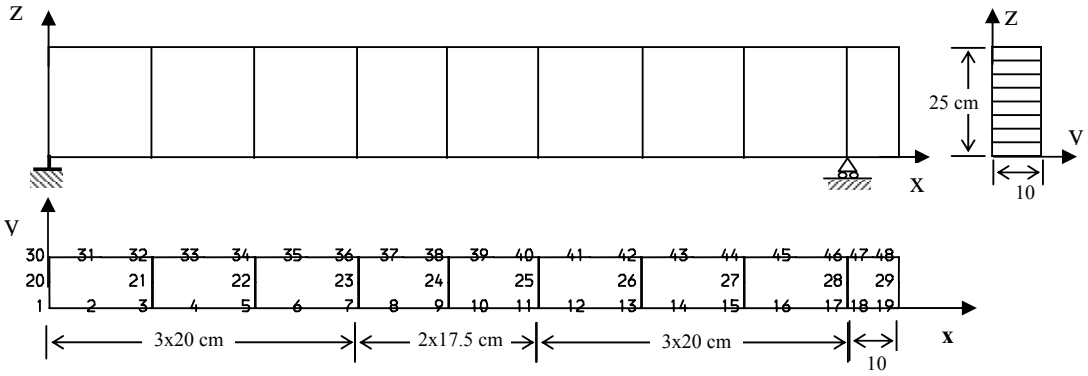

(a) Boundary conditions and mesh of bending stress elements
(9 bending stress elements,48 nodes)

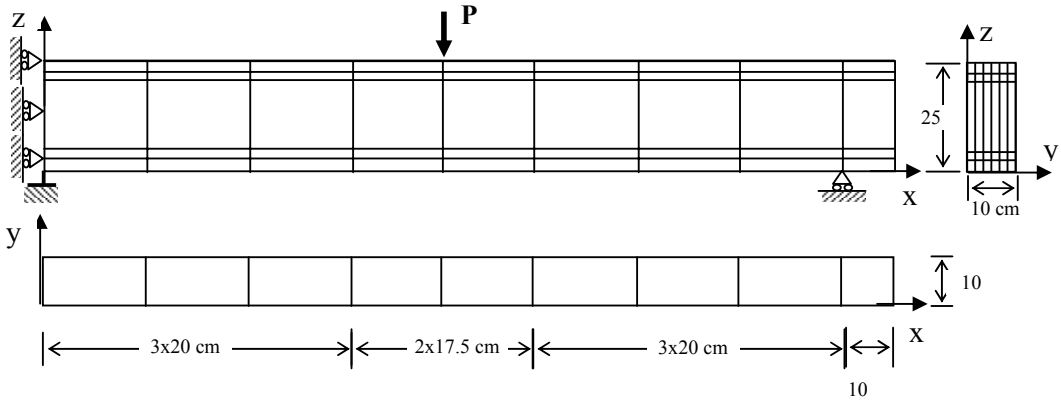

(b) Boundary conditions and mesh of plane stress elements
(45 plane stress elements, 164 nodes)

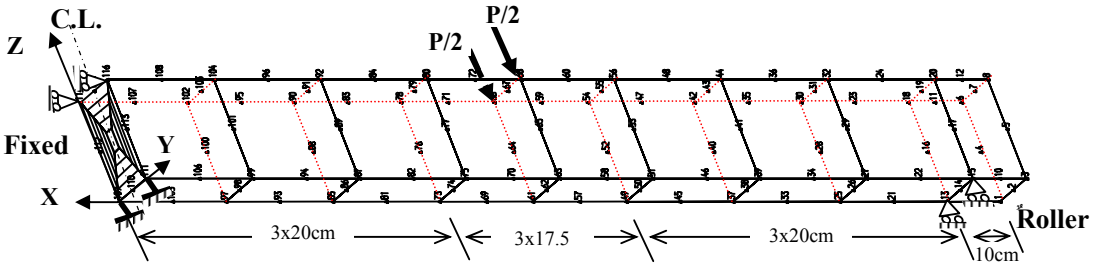

(c) Boundary conditions and mesh of the new compound elements
(9 new compound elements, 36 sub-elements, 116 nodes)

Fig. 13. Boundary conditions and different FEM meshes

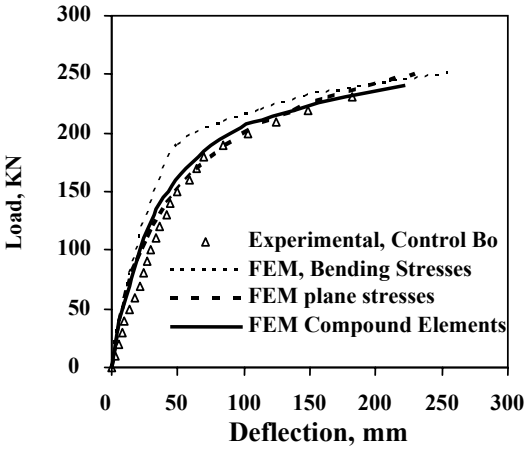

Fig. 14. Comparison between load deflection curves for control beam Bo, Case(a)

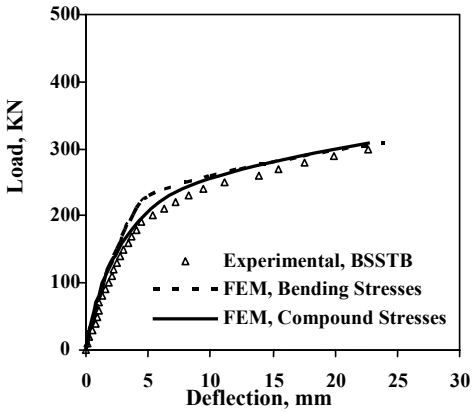

Fig. 15 Load deflection curves for beam BSSTB, Case (b)

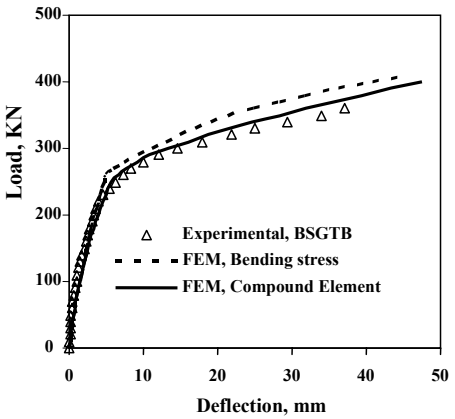

Fig. 16 Load deflection curves for beam BSGTB, Case (b)

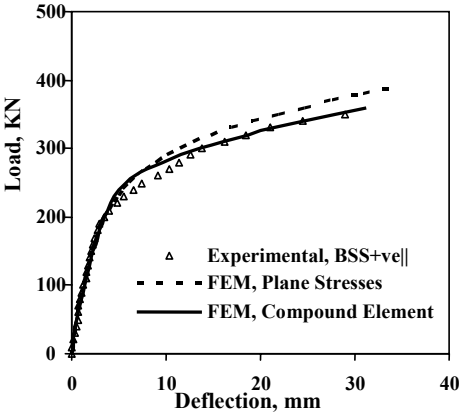

Fig. 17 Load deflection curves for beam BSS+ve||, Case (c)

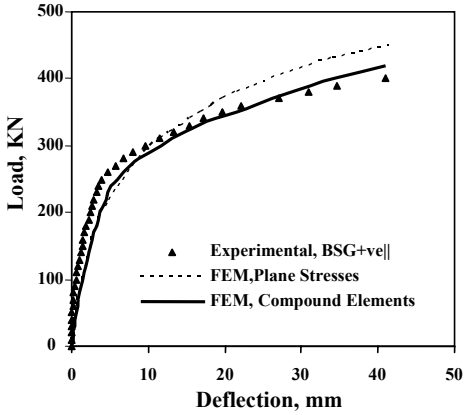

Fig. 18 Load deflection curves for beam BSG+ve||, Case (c)

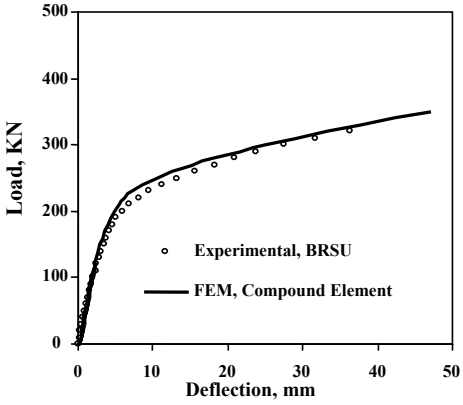

Fig. 19 Load deflection curves for beam BRSU, Case (d)

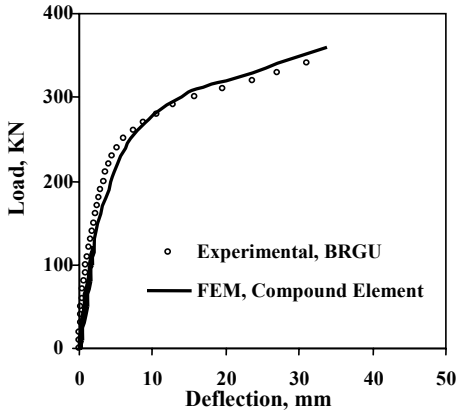

Fig. 20 Load deflection curves
for beam BRGU, Case (d)

References

[1] Zienkiewicz, O.C. and Taylor, R.L. The Finite Element Method. McGraw-Hill, London, 1989.

[2] Hinton, E. and Owen, D.R.J. Finite Elemente Programme. für Platten und Schalen.

Springer-Verlag, Berlin, 1990.

[3] Nilson, A.H. Finite element Analysis of Reinforced Concrete. State of the Art Report, American Society of Civil Engineers. New York. 1982.

[4] Zhang, Y.G. Lu, M.W., and Hwang, K.C. Finite Element Modeling of Reinforced Concrete Structures. Finite Elements in Analysis and Design. 29, 2005.

[5] Owen, D.R.J and Hinton, E. Finite Element in plasticity. Pine ridge Press Limited, Swansea, U.K., 1986.

[6] Ramaswamy, A., Barzegar, F., and Voyiadjis, G.Z. Study of Layering Procedures in Finite Element Analysis of RC Flexural and Torsional Elements. Journal of Structural Engineering, December, 1995.

[7] Elabouky, S.K. Repair and Strengthening of Continuous Reinforced Concrete Beams Using Advanced Materials. Ph.D, Thesis Faculty of Engineering, Minoufiya University, Egypt, 2007.

[8] Heiza, Kh. M. Flexural Behavior of Self-Compacted Reinforced Concrete Beams Strengthened with Hybrid FRP and Steel Systems. Engineering Research Journal, Vol.28,No.1,pp 107-128, January, 2005.

[9] Meleka, N. N., and Tayel M. A. Nonlinear Finite Element Analysis of Reinforced Concrete Members Using Three Dimensional Isoparametric Brick Elements with Embedded Steel Reinforcement. 3rd Alexandria conference on structural and Geotechnical Engineering, Egypt, 1997.

[10] Meleka, N.N. New Compound Finite Element for the Analyses of RC Members Strengthened by External Layers. proceeding of the fourth ERD6 conference, faculty of engineering shebin El-Kom center of rural development, Egypt 2007.

[11] Kupfer, H.B. and Gerstle, K.H. Behavior of Concrete under Biaxial Stresses. Journal of the Eng. Mech. Division, ASCE, Vol. 99, No. EM4, August 1973.

[12] Heiza, Kh. M., N. Meleka, M. Tayel and N. Farah. Behavior of High Strength Reinforced Concrete Flat Slabs Using Nonlinear Finite Element Analysis. Engineering research journal, Vol. 28, No.1, pp79-93 January 2005.

[13] Heiza, Kh. M. Experimental Behavior of Repaired and Strengthened Self-Compacted RC Continues Beams. International conference, excellence in concrete construction – through innovationKingston U.K., 9-10 September 2008.